JOC The Journal of Organic Chemistry

pubs.acs.org/joc Article

Reaction of Nitroxyl (HNO) with Hydrogen Sulfide and Hydropersulfides

Jessica Zarenkiewicz,[†] Vinayak S. Khodade,[†] and John P. Toscano*

Cite This: J. Org. Chem. 2021, 86, 868−877 Read Online

ACCESS | Metrics & More | Article Recommendations | Supporting Information

ABSTRACT: Nitroxyl (HNO) has gained a considerable amount of attention because of its promising pharmacological effects. The biochemical mechanisms of HNO activity are associated with the modification of regulatory thiol proteins. Recently, several studies have suggested that hydropersulfides (RSSH), presumed signaling products of hydrogen sulfide (H_2S)-mediated thiol (RSH) modification, are additional potential targets of HNO. However, the interaction of HNO with reactive sulfur species beyond thiols remains relatively unexplored. Herein, we present characterization of HNO reactivity with H_2S and RSSH. The reaction of H_2S with HNO leads to the formation of hydrogen polysulfides and sulfur (S_8), suggesting a potential role in sulfane sulfur homeostasis. Furthermore, we show that hydropersulfides are more efficient traps for HNO than their thiol counterparts. The reaction of HNO with RSSH at varied stoichiometries has been examined with the observed production of various dialkylpolysulfides (RSS_nSR) and other nitrogen-containing dialkylpolysulfide species ($RSS{-}NH{-}S_nR$). We do not observe evidence of sulfenylsulfinamide ($RS{-}S(O){-}NH_2$) formation, a pathway detected by analogy with the known reactivity of HNO with thiol.

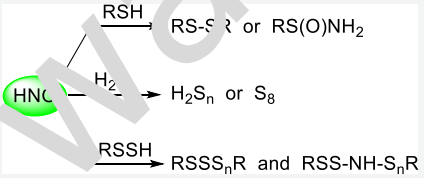

1. INTRODUCTION

Nitroxyl (HNO), the one-electron reduced and protonated form of nitric oxide (NO), is a potential therapeutic for several conditions, including heart failure, alcoholism, vascular dysfunction, and cancer.[1−4] HNO shows a chemical and biological profile distinct from that of NO. One of the important chemical properties of HNO is its electrophilicity toward soft nucleophiles like thiols (RSH).[5] The chemical biology of HNO indicates that thiols and related species are likely targets for HNO-mediated biological activity.[6−8] It has been reported that the reaction of HNO with thiols is relatively fast (k = 2 to 20 × 10^6 M^{-1} s^{-1}) and thermodynamically favorable.[9,10] The reaction of HNO with thiols proceeds via initial attack of the thiol sulfur atom on the electrophilic nitrogen of HNO, giving a short-lived *N*-hydroxysulfenamide ($RS{-}NH{-}OH$) intermediate (Scheme 1).[6,7,11] At low thiol concentrations, this intermediate rearranges to a sulfinamide ($RS(O)NH_2$), presumably via dehydration of the protonated *N*-hydroxysulfenamide intermediate to form an alkyliminosulfonium intermediate followed by reaction with water (Scheme 1, Path A). However, at high thiol concentrations, the *N*-hydroxysulfenamide intermediate reacts with thiol to produce a disulfide (RSSR) and hydroxylamine (NH_2OH) (Scheme 1, Path B). HNO-mediated oxidation of protein thiols to disulfides is considered a biologically reversible modification because disulfides are readily reduced to thiols in the presence of biological reductants. However, oxidation to $RS(O)NH_2$ represents a modification more difficult to reverse in a biological setting.[12]

In the last decade, hydrogen sulfide (H_2S) has emerged as a cell signaling molecule along with NO and carbon monoxide.[13] In mammals, H_2S is produced enzymatically mainly via three enzymes: cystathionine γ-lyase (CSE), cystathionine β-synthase (CBS), and 3-mercaptopyruvate sulfurtransferase.[14,15] H_2S is capable of influencing a myriad of physiological functions.[16−19] In aqueous solution, H_2S (pK_a = 6.98) is in equilibrium with its deprotonated HS^- form,[20] which predominates under physiological conditions (pH 7.4). Despite the involvement of H_2S in various physiological processes, the biochemical mechanisms by which it elicits different responses remain largely unknown. Oxidative post-translational modification of protein cysteine residues to hydropersulfides (RSSH) has been proposed as a significant pathway for H_2S-induced biological effects.[21] Indeed, recently it has been postulated that at least a part of the biological

Scheme 1. Reaction of HNO with Thiols

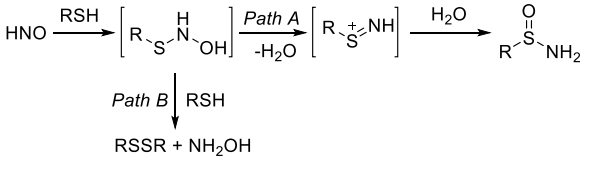

Received: October 11, 2020
Published: December 22, 2020

https://dx.doi.org/10.1021/acs.joc.0c02412
J. Org. Chem. 2021, 86, 868−877

activities of H_2S is attributed to the generation of RSSH rather than H_2S itself.[21−23] Recent advances in analytical methods revealed the prevalent nature of small molecule and protein RSSH in biological systems. For example, Ida and co-workers reported that mammalian tissues contain >100 μM of glutathione hydropersulfide (GSSH).[24] Likewise, significant levels of cysteine hydropersulfide (Cys-SSH) are also present in cells.[24] Furthermore, cysteine residues in a variety of proteins/enzymes have been reported to be modified to the corresponding hydropersulfide. For example, 10−25% of proteins in mouse liver lysate are persulfidated under physiological conditions.[21] Three enzymes, CSE, CBS, and cysteinyl-tRNA synthetases, have been reported to catalyze the formation of Cys-SSH.[24,25] Interestingly, RSSH display distinct chemical properties that may be relevant to their biology. For example, RSSH are more acidic than the corresponding RSH. Everett and co-workers have estimated the pK_a of 2-[(3-aminopropyl)amino]ethane hydropersulfide to be 6.2, which is 1.6 units lower than the corresponding thiol.[26] The pK_a of cysteine hydropersulfide was computationally estimated to be ∼4 units lower than that of the cysteine.[27] More recently, Alvarez and co-workers reported the pK_a of GSSH to be 5.45, which is 3.49 units lower than GSH.[28] These results indicate that a higher ratio of RSS^-/RSSH compared with RS^-/RSH under physiological conditions. Additionally, RSSH have greater reducing potential than the corresponding RSH.[29−31] Also, RSSH are more nucleophilic than the corresponding RSH,[27,28,30] presumably because of the alpha effect.

The ability of HNO to target thiols and thiol-containing proteins makes it likely that small molecule and protein hydropersulfides are additional potential targets for HNO. While the reaction of HNO and various thiols has been well characterized, the reaction between HNO and other reactive sulfur species such as H_2S and RSSH remains relatively unexplored. Being highly thiophilic, HNO is expected to react with H_2S as well as with RSSH. Indeed, it has been proposed that the specificity of HNO signaling may be a function of the presence of cysteine hydropersulfide residues in proteins.[8] This suggestion is consistent with the idea that HNO may react preferentially with RSSH because RSSH have enhanced nucleophilicity and reducing capability. Indeed, Fukuto and co-workers have demonstrated the interaction between RSSH and HNO,[32] although the chemical details of this reaction remain to be further elucidated. Herein, we present characterization of HNO reactivity toward H_2S and RSSH along with a comparison of this reactivity with RSH.

2. RESULTS AND DISCUSSION

2.1. Reactivity of HNO with H_2S. Because of HNO's inherent reactivity, it must be generated in situ. We used Angeli's salt (AS, $Na_2N_2O_3$) as a HNO donor.[33] AS decomposes spontaneously under physiological conditions via protonation of the dianion to produce equimolar amounts of nitrite and HNO with a half-life of about 2.4 min at 37 °C.[34] In the absence of chemical traps, HNO rapidly dimerizes ($k = 8 \times 10^6$ M^{-1} s^{-1}) and dehydrates to form nitrous oxide (N_2O).[33] However, addition of a chemical trap such as thiol competes with HNO dimerization leading to a reduction in N_2O yield. The inorganic salt, sodium sulfide (Na_2S), was used as the source of H_2S.

Initially, we examined the reaction of HNO with H_2S by membrane inlet mass spectrometry (MIMS). This technique can monitor the relative amounts of small hydrophobic gases dissolved in aqueous solution using a semipermeable membrane that allows the dissolved gases, but not water, to enter a mass spectrometer.[35−37] When AS (500 μM) is incubated with H_2S (100 μM) in pH 7.4 phosphate-buffered saline (PBS) under anaerobic conditions, a reduction in the signal corresponding to the HNO dimerization product N_2O (m/z = 44) is observed (Figure 1a). Consistent with this observation, a reduction in the signal corresponding to H_2S (m/z = 34) is also observed (Figure 1b), confirming that H_2S reacts with HNO.

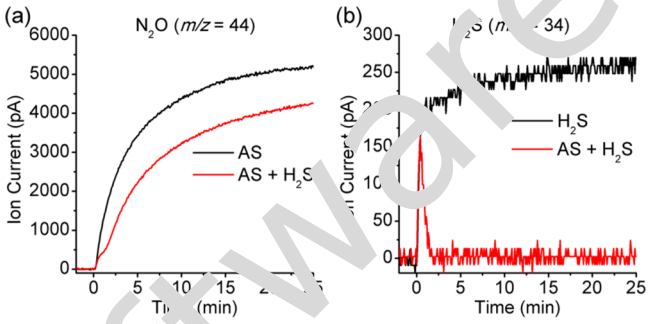

Figure 1. M[illegible]S signal observed at (a) m/z = 44 corresponding to N_2O^+ and (b) m/z = 34 corresponding to H_2S^+ during incubation of AS (500 [illegible]) and H_2S (100 μM) alone or together in argon-purged PBS (pH 7.4, 100 mM) containing the metal chelator DTPA (100 μM) at 37 °C.

To verify the reaction between HNO and H_2S, we independently analyzed the yield of N_2O by gas chromatography (GC) headspace analysis. For comparison, analogous experiments were conducted with *N*-acetylcysteine methyl ester (pK_a = 7.28) because of its similar pK_a to H_2S (pK_a = 6.98).[20] As the thiolate anion is the active species in this reaction, thiol concentrations were adjusted such that equal amounts of thiolate anion were present in solution. Incubations of AS (200 μM) with varying concentrations of H_2S show a marked decrease in N_2O production relative to AS only (Figure 2, black bars). Similarly, addition of *N*-acetylcysteine methyl ester to buffer solutions containing AS also results in a decrease in N_2O production (Figure 2, red bars). Quantification of the N_2O yields reveals that H_2S is a more efficient trap

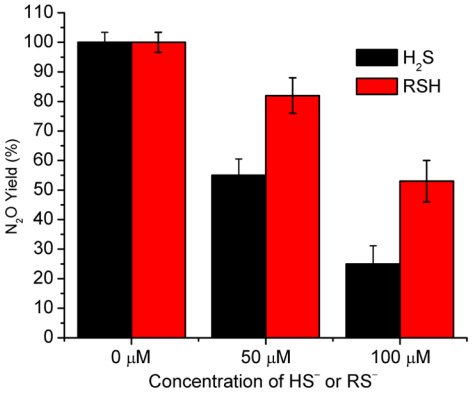

Figure 2. GC-determined relative yields of N_2O in the presence of increasing concentrations of HNO trap, H_2S (black bars), or *N*-acetylcysteine methyl ester (red bars). Incubations were performed with 0, 50, and 100 μM HS^- or RS^- and 200 μM AS in phosphate buffer (pH 7.4, 100 mM) with DTPA (100 μM) at 37 °C for 3 h.

https://dx.doi.org/10.1021/acs.joc.0c02412
J. Org. Chem. 2021, 86, 868−877

for HNO compared with *N*-acetylcysteine methyl ester. In addition, a comparison between H_2S and thiophenol (PhSH) reactivity with HNO reveals that H_2S is likewise a better trap for HNO compared with PhSH (Supporting Information, Figure S1).

After confirming HNO trapping by H_2S, we examined the mechanism of this reaction. Based on previous reports on the reaction of HNO with thiols, we expected that the HNO reaction with H_2S should proceed via the intermediacy of *N*-mercaptohydroxylamine **1** (HSNHOH), and depending on the relative concentrations of H_2S, this intermediate would either produce hydrogen disulfide (H_2S_2) and NH_2OH (Scheme 2,

Scheme 2. Proposed Mechanism of HNO Reaction with H_2S

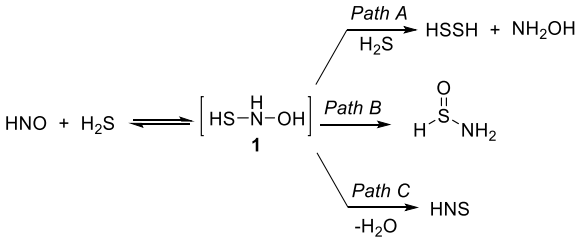

Path A) or sulfinamide (Scheme 2, Path B). In addition, the *N*-mercaptohydroxylamine intermediate might also undergo dehydration to yield thionitrosyl hydride (HNS) (Scheme 2, Path C).

First, we analyzed the products of this reaction under conditions of excess H_2S. We anticipated that if the *N*-mercaptohydroxylamine intermediate **1** reacts further with H_2S, we should observe H_2S_2 and NH_2OH (Scheme 2, Path A). We examined H_2S_2 generation by trapping with *β*-(4-hydroxyphenyl)ethyl iodoacetamide (HPE-IAM) (Scheme 3).

Scheme 3. Polysulfide Trapping with HPE-IAM to Produce Bis-$(S)_n$-HPE-AM

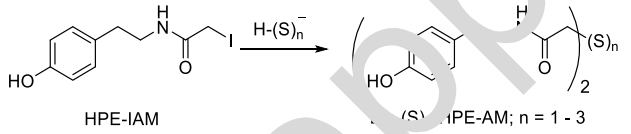

HPE-IAM was chosen because it is a soft electrophile and has been shown to be relatively resistant toward electrophile-mediated decomposition of longer chain polysulfides,[38,39] if they are formed. As expected, ultraperformance liquid chromatography–mass spectrometry (UPLC–MS) analysis of H_2S incubation with HPE-IAM shows thioether bis-S-HPE-AM formation as a major product (Figure 3a, bottom trace). However, analogous analysis of H_2S (4 equiv) incubation with HNO shows a significant increase in bis-SS-HPE-AM formation with concomitant decrease in bis-*S*-HPE-AM (Figure 3b), consistent with H_2S_2 generation. In addition, a small amount of bis-SSS-HPE-AM is also observed, presumably produced by disproportionation of H_2S_2 to H_2S_3 and H_2S. Interestingly, no longer-chain polysulfides are observed under these conditions. We also examined NH_2OH formation, another anticipated product of HNO reaction with excess H_2S (Scheme 2, path A), by derivatization with 4-cyanobenzaldehyde. High-performance liquid chromatography (HPLC) analysis shows 4-cyanobenzaldehyde oxime formation

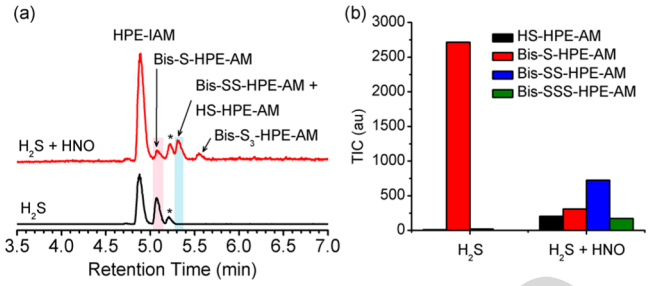

Figure 3. (a) Analysis of polysulfides generated from the H_2S reaction with HNO. AS (25 μM) was incubated with Na$_2$S (100 μM) in pH 7.4 ammonium bicarbonate buffer (25 mM) containing DTPA (100 μM) at 37 °C. After 15 min, an aliquot of the reaction mixture was withdrawn and incubated with HPE-IAM (1 mM) for 15 min. The asterisk indicates the presence of impurity in the commercial HPE-IAM sample. HS-HPE-AM coelutes with bis-SS-HPE-AM under these conditions. (b) A comparison of sulfur species (e.g., H_2S, H_2S_2, and H_2S_3) measured by detection of the trapped HPE-AM species from H_2S alone vs H_2S reaction with HNO.

(Supporting Information, Figure S7), confirming NH_2OH generation under these conditions.

We then analyzed the reaction of H_2S with excess HNO, analogous to previously studied thiol–HNO reactions, which primarily result in sulfinamide formation.[4] Incubation of H_2S with excess HNO (4 equiv) results in a purple solution that turns colorless within 5 min with concomitant formation of a white precipitate. We speculate that the white solid formed under these conditions is S_8. To explore this possibility, we analyzed for S_8 by a triphenylphosphine (PPh_3)-based ^{31}P NMR assay. PPh_3 is known to react with S_8 to form triphenylphosphine sulfide (S=PPh_3), which can be detected by ^{31}P NMR spectroscopy.[40] We extracted the white precipitate formed during the reaction of H_2S with excess HNO in $CDCl_3$ and incubated with PPh_3. ^{31}P NMR analysis of this mixture shows a new peak at 43.3 ppm (Figure 4b), indicating S_8 generation under these conditions. The same species is also generated from the reaction of authentic S_8 with PPh_3 (Figure 4a). Based on a calibration curve generated from the reaction of known

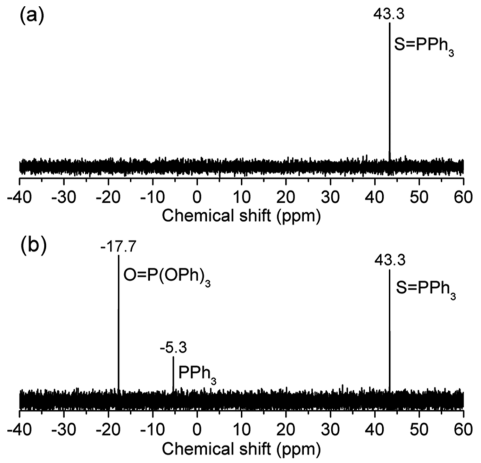

Figure 4. Selected region of the ^{31}P NMR spectra following incubation of (a) authentic S_8, and (b) the white precipitate produced during the reaction of H_2S (5 mM) with HNO (20 mM) extracted in $CDCl_3$ with PPh_3 (−5.3 ppm). S=PPh_3 is observed at 43.3 ppm. The peak at −17.7 ppm corresponds to triphenyl phosphate (O=$P(OPh)_3$), which is used as an internal standard.

https://dx.doi.org/10.1021/acs.joc.0c02412
J. Org. Chem. 2021, 86, 868–877

amounts of commercially available elemental sulfur (S_8) with PPh_3, we determined the S_8 yield to be approximately 79% of the sulfur introduced into the reaction mixture. To verify S_8 generation, the white solid was independently analyzed by electron ionization (EI)-MS. As anticipated, a new peak with m/z = 257.8 (expected m/z = 257.5) is observed (Supporting Information, Figure S8), confirming S_8 generation.

Two pathways can be envisioned for S_8 generation under conditions of H_2S reaction with excess HNO (Scheme 4). As

Scheme 4. Proposed Mechanism of S_8 Generation from H_2S Reaction with Excess HNO

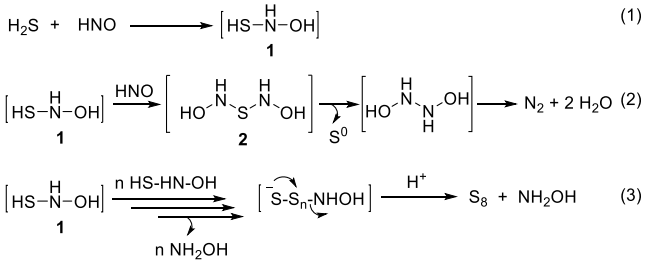

shown in Scheme 4, eq 2, reaction of the initial *N*-mercaptohydroxlamine intermediate **1** with a second equivalent of HNO would lead to the formation of intermediate **2**. This pathway is supported by our GC data (Figure 2) in which H_2S incubation with 4 equiv of HNO shows nearly 2 equiv of HNO trapping, supporting that intermediate **1** reacts with a second equivalent of HNO to produce intermediate **2**. We propose that intermediate **2** can undergo a sulfur extrusion reaction to generate S_0 and dihydroxyhydrazine, which then decomposes to produce nitrogen (N_2) and water.[41] To test this hypothesis, we analyzed for N_2 generation using MIMS. Incubation of H_2S under conditions of excess HNO shows increase in the m/z = 28 signal (Figure 5) indicating N_2

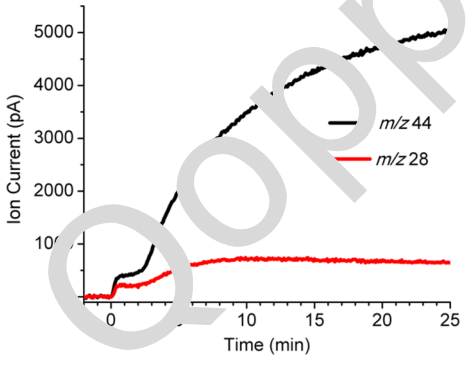

Figure 5. MIMS signals observed at m/z = 44 corresponding to N_2O^+ and m/z = 28 corresponding to a combination of N_2O fragmentation to N_2^+ and N_2 generated from the reaction of H_2S with excess HNO.

generation. However, the detection of N_2 is complicated by N_2O (m/z = 44) fragmentation, which also generates an m/z = 28 signal (Supporting Information, Figure S2). Hence, we compared the ratio of 44:28 signals from AS alone with that for AS + H_2S. The 44:28 ratio for N_2O alone produced from AS decomposition was found to be 9.5:1 (Supporting Information, Figure S3). This result is consistent with the NIST reported a 44:28 ratio of 9.25:1 for the EI mass spectrum of N_2O.[42] In contrast, MIMS monitoring of the H_2S reaction with excess HNO results in a 44:28 ratio that varies from 2:1 at early time points to 8:1 at the 25 min mark (Supporting Information, Figure S3). These results suggest another contributor to the m/z = 28 signal, which we attribute to N_2. The variation in the 44:28 ratio over the course of the experiment suggests that N_2 is generated at early times and decreases as the experiment progresses.

We independently examined the H_2S reaction with excess HNO using 2-bromo-Piloty's acid (2-BrPA). In aqueous solution, 2-BrPA produces HNO and 2-bromophenylsulfinic acid as a byproduct.[38] Incubation of H_2S with 2-BrPA (4 equiv) in pH 7.4 PBS again shows the formation of S_8 and N_2 (Supporting Information, Figures S4 and S9). This result confirms that nitrite, a byproduct of AS decomposition, is not involved in S_8 and N_2 formation during the H_2S reaction with excess HNO.

Alternatively, S_8 can also be produced via disproportionation of the *N*-mercaptohydroxlamine intermediate **1** followed by intramolecular cyclization as shown in Scheme 4, eq 3. However, HPE-IAM trapping studies at early time points, before the formation of the white precipitate, show that no longer-chain polysulfides are formed (Supporting Information, Figure S15), indicating that the proposed mechanism in Scheme 4, eq 3 is likely not operative under these conditions. Furthermore, intermediate **1** could also undergo homolytic cleavage to produce hydrosulfide radicals ($HS^\bullet$), which can lead to higher order sulfur species in a process catalyzed by either trace metals or residual oxygen present in solution.[43] However, we do not observe changes in the S_8 yield from the HNO reaction with H_2S under aerobic versus anaerobic conditions (Supporting Information, Figure S10). In addition, the presence or lack of a metal chelator diethylenetriaminepentaacetic acid (DTPA) in solution also does not influence the final products of the reaction, indicating that $HS^\bullet$ is likely not involved in this reaction.

Based on the significant S_8 formation observed under conditions of excess HNO, it appears that sulfinamide formation is not a major pathway under these conditions; however, more studies are required. In addition, as suggested in Scheme 2, Path C, the *N*-mercaptohydroxylamine intermediate **1** could undergo dehydration to yield HNS. If formed, HNS may undergo further reaction, similar to HNO, yielding N_2S and H_2S. However, MIMS analysis shows no evidence of HNS or N_2S formation under conditions of either excess HNO or H_2S (Supporting Information, Figure S5), indicating that this reaction pathway is presumably not operative. Taken together, our results indicate that H_2S reacts with HNO to produce either short-chain hydrogen polysulfides (H_2S_n) or S_8 depending on their relative concentrations. With excess H_2S, H_2S_n formation is favored (Scheme 2, Path A). In contrast, S_8 is produced under conditions of excess HNO (Scheme 4, eqs 1 and 2).

2.2. Reactivity of HNO with Hydropersulfides. The propensity of RSSH to undergo decomposition under aqueous conditions precludes convenient and direct accessibility of RSSH for chemical and biological studies. Hence, donor molecules capable of releasing RSSH in situ are needed. We utilized our recently developed alkylamine-substituted perthiocarbamate **3a** as a primary alkyl RSSH donor, and **3b** as a tertiary alkyl RSSH donor (Scheme 5).[44] At physiological pH, these precursors release RSSH and 1,3-dimethyl-2-imidazolidinone (**4**) as a byproduct (Scheme 5, eq 1). In the absence of trapping agents, RSSH reacts with the precursor producing dialkyltrisulfide (S_3) and a thiocarbamate intermediate

https://dx.doi.org/10.1021/acs.joc.0c02412
J. Org. Chem. 2021, 86, 868−877

Scheme 5. RSSH Release from Precursors 3a and 3b

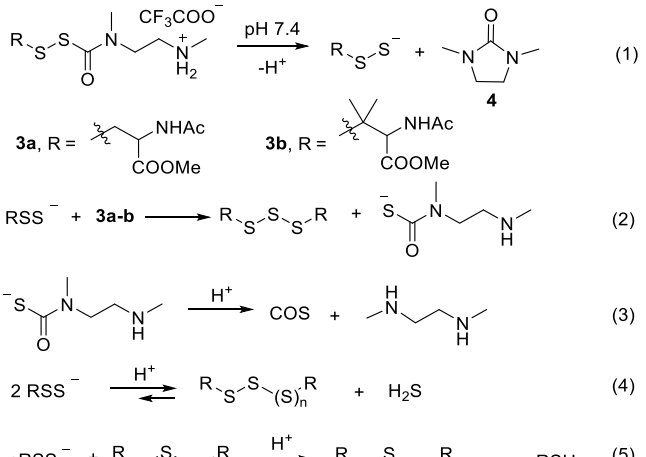

(Scheme 4, eq 2), which rapidly decomposes to release carbonyl sulfide (COS) (Scheme 5, eq 3). In addition, RSSH also undergoes disproportionation reactions to produce dialkylpolysulfides (Scheme 5, eqs 4 and 5).[44]

Initially, the reaction of HNO with RSSH was examined by MIMS. Incubation of AS (100 μM) with **3a** (25 μM) in PBS (pH 7.4) shows a reduction in the signal corresponding to N_2O (m/z = 44) (Figure 6a), indicating that RSSH reacts with

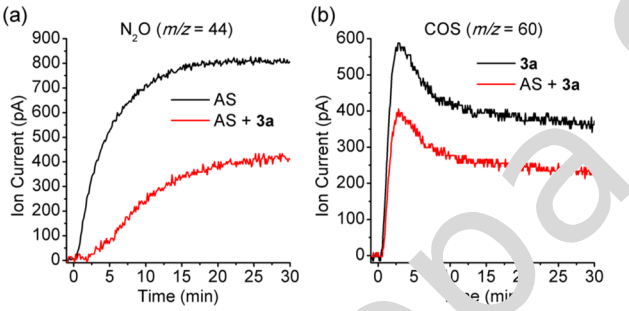

Figure 6. MIMS signals observed at (a) m/z = 44 corresponding to N_2O^+ during incubation of either AS (100 μM) alone or with RSSH precursor **3a** (25 μM), and (b) m/z = 60 corresponding to COS^+ during incubation of either RSSH precursor **3a** (25 μM) alone or with AS (100 μM) in argon-purged PBS (pH 7.4, 100 mM) containing DTPA (100 μM) at 37 °C.

HNO. In addition, a reduction in the signal attributed to COS (m/z = 60) is also observed (Figure 6b), also supporting that RSSH reacts with HNO, and as a result it is less available to react with precursor **3a** itself to produce dialkyltrisulfide (S_3) and thiocarbamate-derived COS (Scheme 5, eqs 2 and 3). Analogous experiments with precursor **3b** also show HNO trapping (Supporting Information, Figure S6), albeit better than **3a** presumably because of the sterically hindered disulfide bond in precursor **3b** inhibiting its reaction with released RSSH.

The ability of RSSH to react with HNO was independently analyzed by GC headspace analysis. A thiol comparison was used to examine the nucleophilicity of RSSH. We began by determining the pK_as of *N*-acetylcysteine methyl ester (**5a**, pK_a = 7.28) and *N*-acetylpenicillamine methyl ester (**5b**, pK_a = 7.02). Because of the unstable nature of RSSH in the deprotonated state, there is not a reliable way to determine their pK_a. We assumed a pK_a difference of 1.5 units for this study. With this assumption, the hydropersulfide is 98% deprotonated at physiological pH. After correcting for differences in pK_a, we find that RSSH (**3a** and **3b**) are better traps for HNO than their thiol counterparts (**5a** and **5b**) (Figure 7). Additionally, **3b** exhibited better HNO-trapping

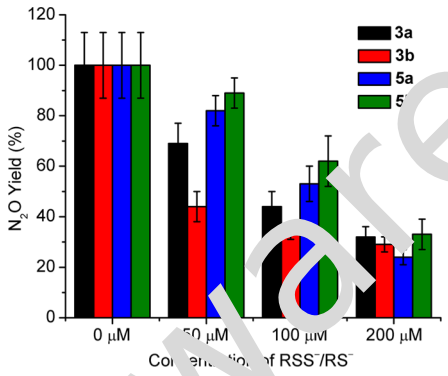

Figure 7. GC-determined relative yield of N_2O in the presence of increasing concentrations of **3a** (black bars), **3b** (red bars), *N*-acetylcysteine methyl ester (**5a**, blue bars), and *N*-acetylpenicillamine methyl ester (**5b**, green bars). Incubations were performed with 0, 50, 100, and 200 μM RSSH$^-$ or RS$^-$ and 200 μM AS in PBS (pH 7.4, 100 mM) with DTPA (100 μM) at 37 °C for 3 h.

efficiency than **3a**, likely because of competitive RSSH trapping by the sterically accessible disulfide bond in the precursor **3a** itself. We note that even if the pK_a of RSSH is 4 units lower than the corresponding thiol, the RSSH anion concentration would be 99.9% (rather than 98%) under the conditions of our experiments, a negligible impact on the RSSH concentrations employed.

Next, we studied the mechanism of this reaction. Based on the known thiol−HNO reaction, a variety of outcomes for the reaction between RSSH and HNO are possible. The initial reaction of HNO with RSSH is expected to proceed through an *N*-hydroxy-perthiosulfenamide (RSS−NH−OH) intermediate **6** (Scheme 6). As with thiols, we anticipate that the concentration of RSSH relative to that of HNO will play an important role in the nature of the observed products.

Initially, **3a** decomposition was examined in the absence of HNO by UPLC−MS. Incubation of **3a** in pH 7.4 buffer shows dialkyldisulfide (labelled as S_2) generation as a major product (Figure 8a, bottom trace). In addition, a small amount of dialkyltrisulfide, dialkyltetrasulfide, dialkylpentasulfide, and

Scheme 6. Proposed Mechanism of HNO Reaction with RSSH

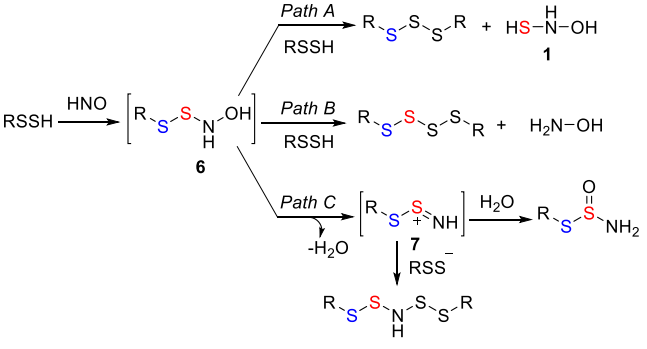

https://dx.doi.org/10.1021/acs.joc.0c02412
J. Org. Chem. 2021, 86, 868−877

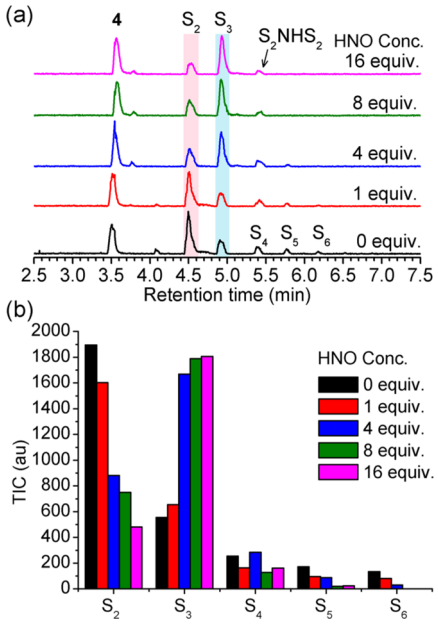

Figure 8. (a) UPLC−MS chromatograms of primary alkyl hydropersulfide precursor **3a** (50 μM) incubated without and with increasing concentrations of AS (50, 200, 400, and 800 μM) in ammonium bicarbonate buffer (pH 7.4, 25 mM) containing DTPA (100 μM) at 37 °C for 15 min, followed by quenching in 1% formic acid. RSSH-derived symmetrical dialkyl polysulfide, labeled as S_2 to S_6 (RSS_nSR, n = 0−4) formation is evident. A peak at 3.52 min attributed to the byproduct **4** is also observed. A small peak at 5.4 min corresponding to RSS−NH−SSR coelutes with S_4. (b) Comparison of RSSH-derived symmetrical dialkyl polysulfide, labelled as S_2 to S_6 (RSS_nSR, n = 0−4) from the **3a** and **3a** + AS reaction mixtures.

dialkylhexasulfide (labeled as S_3, S_4, S_5, and S_6, respectively) formation is also observed, presumably via RSSH disproportionation reactions (Scheme 5, eqs 4 and 5). In contrast, when **3a** is incubated with AS (1 equiv), a slight decrease in S_2 with a concomitant increase in S_3 is observed (Figure 8b). Furthermore, as the ratio of AS to **3a** is increased, an increase in the relative amount of S_3 with concomitant decrease in S_2 is observed. These results suggest that RSSH indeed reacts with HNO to produce intermediate **7**, which reacts further with RSSH producing S_3 and *N*-mercaptohydroxylamine intermediate **1** (Scheme 6, Path A). The intermediate **1** might react further with RSSH to produce RSSSH. Consistent with this observation, we also observe reduced levels of S_4, S_5, and S_6 with increasing concentrations of AS, demonstrating that RSSH traps HNO and thus it is less available to undergo disproportionation reactions to produce longer-chain polysulfides. Alternatively, RSSH can also react with the external sulfur of intermediate **6** to produce S_4 and NH_2OH (Scheme 6, Path B). However, a lack of major change in the S_4 concentration with increasing concentration of HNO suggests that Path B is likely not operative under these conditions, presumably because of the sterically accessible internal sulfur atom of intermediate **6** being available to react with RSSH to produce S_3. We anticipated that the intermediate **6** might rearrange to sulfenylsulfinamide ($RS{-}S(O){-}NH_2$) under conditions of excess HNO (Scheme 6, Path C). However, UPLC−MS analysis shows no evidence of its formation. Instead, a minor new peak at 5.4 min with m/z = 454.0199 is observed (Supporting Information, Figure S22). We assign this new peak to RSS−NH−SSR (Figure 8a, labeled as S_2NHS_2).

These results suggest that intermediate **6** undergoes dehydration to produce the intermediate **7** (Scheme 6, Path C), which can be trapped either by water to produce $RS{-}S(O){-}NH_2$ or by RSSH to produce RSS−NH−SSR. The lack of $RS{-}S(O){-}NH_2$ formation does not exclude its formation because it can react further with RSSH under these conditions to produce S_3.

We also examined the HNO reaction with the tertiary alkyl RSSH precursor **3b**. UPLC−MS analysis of **3b** incubation in the absence of HNO shows a peak at 5.67 min corresponding to RSSH as well as polysulfides (RSS_nSR, n = 1−4) and *N*-acetylpenicillamine methyl ester (**5b**) (Figure 9a, bottom

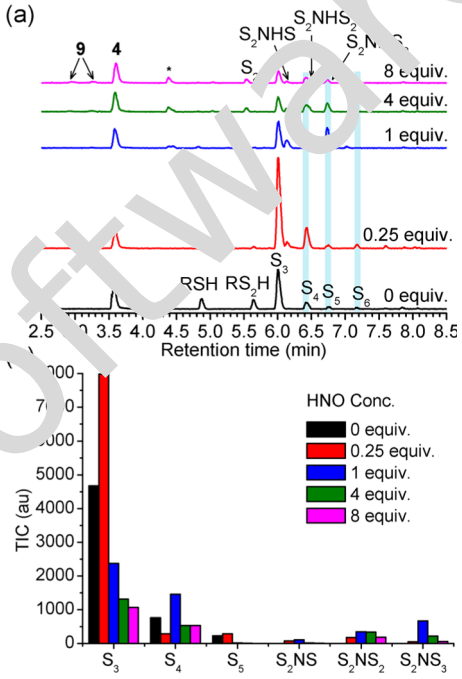

Figure 9. (a) UPLC−MS chromatograms of tertiary alkyl hydropersulfide precursor **3b** (50 μM) incubated without and with increasing concentrations of AS in ammonium bicarbonate buffer (pH 7.4, 25 mM) containing DTPA (100 μM) at 37 °C for 15 min, followed by quenching in 1% formic acid. RSSH-derived symmetrical dialkylpolysulfide, labelled as S_3 to S_6 (RSS_nSR, n = 1−4), formation is evident. A peak at 3.52 min attributed to the byproduct **4** is also observed. The asterisk indicates an unknown product. (b) Comparison of RSSH-derived symmetrical dialkylpolysulfide, labeled as S_3 to S_6 (RSS_nSR, n = 1−4) and RSS−NH−S_nR (n = 1−3) from **3b** and **3b** + AS reaction mixtures.

trace). This result indicates that RSSH undergoes disproportionation reactions and its presence is likely because of equilibrium reactions with polysulfides.[44] We then examined the RSSH reaction with HNO under conditions of excess RSSH. When 4 equiv of **3b** is incubated with AS, the peak attributed to RSSH disappears and the level of S_3 increases (Figure 9b, red bars). In addition, small peaks at 6.14, 6.43, and 6.74 min that we ascribe to RSS−NH−SR, RSS−NH−SSR, and RSS−NH−SSSR, respectively (Figure 9a and Supporting Information, Figures S33−S35, labeled as S_2NHS, S_2NHS_2, and S_2NHS_3) are observed, presumably formed by the reaction of intermediate **7** with RSH, RSSH, and RSSSH, respectively. We then examined the **3b** reaction with AS at equimolar concentrations. UPLC−MS analysis shows the reduced level of S_3 and increased levels of S_4 and RSS−

https://dx.doi.org/10.1021/acs.joc.0c02412
J. Org. Chem. 2021, 86, 868−877

NH−S_nR (n = 1−3) (Figure 9b, blue bars). Furthermore, the **3b** reaction was also checked under conditions of excess HNO and we observe reduced levels of polysulfides (S_3, S_4, and S_5) and RSS−NH−S_nR (n = 1−3). In addition, two new minor peaks at 2.9 and 3.3 min with m/z = 205.643 were observed (Figure 9a, top trace and Supporting Information Figures S30 and S31). We assign these peaks to *N*-(2-hydroxy-5,5-dimethyl-3-oxoisothiazolidin-4-yl)acetamide isomers **9**, presumably formed by the intramolecular cyclization of intermediate **8** as shown in Scheme 7. Intermediate **8** can be

Scheme 7. Proposed Mechanism of 9 Formation from the 3b Reaction with Excess HNO

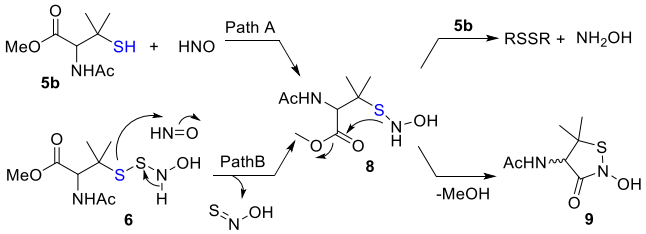

obtained by the HNO reaction with thiol **5b**, produced either by RSSH exchange reactions with RS−S_n−SR or HNO-induced decomposition of intermediate **6** (Scheme 7, Path B). To verify this observation, **5b** was independently incubated with excess HNO and we observe HNO-mediated thiol oxidation to disulfide as a major product (Supporting Information, Figure S36). In addition, similar peaks at 2.9 and 3.3 min were evident in the case of the reaction of **5b** with HNO, suggesting that cyclization product **9** is likely formed during the **3b** reaction with excess HNO.

We predicted that the concentration of RSSH relative to that of HNO would have an important role in the nature of the observed products. However, all conditions studied here indicate that HNO-induced modification of RSSH results in the formation of various dialkylpolysulfides. Interestingly, several unique species such as RSS−NH−R are also observed.

Recently, Pluth and coworkers reported that RSSH react with nitrite to produce NO via inorganic polysulfides and a perthionitrite ($ONSS^-$) intermediate.[45] UV−vis analysis of the $ONSS^-$ intermediate obtained from the reaction of adamantyl persulfide with tetrabutylammonium nitrite in THF exhibits an absorbance at 446 nm. Decomposition of $ONSS^-$ subsequently leads to the formation of NO and inorganic polysulfide. To test if a similar reaction pathway is operative during the reaction of **3b** with AS (which produces nitrite as byproduct), we analyzed this reaction by UV−vis spectroscopy. Incubation of **3b** with AS in pH 7.4 PBS at 37 °C shows no absorption band between 400 and 450 nm (Supporting Information, Figure S43), indicating that $ONSS^-$ is likely not produced under these conditions. We also examined the **3b** reaction with sodium nitrite and UV−vis analysis shows no absorption band between 400 and 450 nm (Supporting Information, Figure S44). We then analyzed NO generation from the reaction of **3b** with AS, and nitrite by GC headspace analysis. We see no evidence of NO generation (Supporting Information, Figure S46), indicating that RSS^- is likely not reacting with nitrite under these conditions. We also examined the RS(S)$_n$H, and HS(S)$_n$H generation during the reaction of **3b** with HNO by trapping with HPE-IAM (Supporting Information, Figure S41). As expected, UPLC−MS analysis shows a significant reduction in RSS-HPE-AM adduct formation during the **3b** reaction with HNO compared with **3b** alone, confirming that RSSH indeed reacts with HNO. However, no evidence of inorganic polysulfide formation is observed, suggesting that RSSH reacts efficiently with HNO and as a result is less available to undergo disproportionation reactions to produce inorganic polysulfides. Taken together, these results indicate that $ONSS^-$ is likely not formed under these conditions.

3. CONCLUSIONS

Reactive sulfur species (RSS) and reactive nitrogen species play diverse and critical roles in cellular signaling and the fundamental chemistry of these species as well as their generation and consumption are critical for understanding their participation in signaling mechanisms. In this work, we first studied the reaction of HNO with H_2S. Our results indicate that H_2S also reacts with HNO to produce either hydrogen polysulfides (H_2S_n) or RSSH depending on their relative concentrations. H_2S_n represents an emerging class of RSS whose presence and potential roles in biological systems are only recently beginning to be appreciated.[46] In addition, comparison of the reactivity of thiol with analogous RSSH shows that RSSH are more potent traps for HNO. These results indicate the specificity of HNO signaling may be a function of reaction with RSSH. Furthermore, HNO reaction with small molecule RSSH produces various RSS$_n$SR and RSS−NH−S$_n$R species with no evidence of RS−S(O)−NH$_2$ under the conditions studied.

4. EXPERIMENTAL PROCEDURES

4.1. General Methods. All chemicals were purchased from commercial sources and used as received unless stated otherwise. NMR spectra were obtained on a 400 MHz FT-NMR spectrometer. All chemical shifts of spectra were reported in parts per million (ppm) relative to tetramethylsilane (δ = 0). The pH measurements were performed using a Fisher Scientific Accumet AB15 pH-meter. Ultraviolet−visible (UV−vis) absorption spectra were obtained using a diode-array spectrophotometer. GC analysis was performed on an instrument equipped with an electron capture detector and Restek column (ShinCarbon ST 80/100, 2m, 1/8″ OD). HPLC was performed on Agilent Technologies 1100 Series, attached with a C-18 column (Hichrom, 5 μm, 4.6 × 150 mm). High-resolution mass spectra were obtained from a Waters Acquity Q-ToF MS/MS instrument. UPLC−MS analysis was carried out with a Waters Acquity/Xevo-G2 UPLC−MS system equipped with ACQUITY UPLC BEH C18 column (2.1 × 50 mm, 1.7 μm). The mass signals for products of polysulfides trapping with HPE-IAM and dialkylpolysulfides were obtained via deconvolution using MassLynx 4.1 software. EI-MS spectra were acquired using a VG-70S Magnetic Sector Mass Spectrometer. To ensure that equal amounts of anion (HS^- and RS^- or RSS^- and RS^-) are present in solution during the reaction of sulfur nucleophiles with HNO, we calculated the concentration of anion using the pK_a of H_2S and thiol/RSSH of interest to determine the percentage of anion present at pH 7.4; pH = pK_a + log(A^-)/(HA)

4.2. Synthesis and Characterization. The HNO donors, Angeli's salt,[47] and 2-bromo-*N*-hydroxybenzenesulfonamide (2-BrPA)[48] were prepared as previously described. Hydropersulfide precursors (**3a** and **3b**), *N*-acetyl-penicillamine methyl ester (**5b**), and 4-cyanobenzaldehyde oxime were synthesized as previously reported, and analytical characterization data were consistent with the reported values.[44,49]

4.3. Analysis of HNO Reaction with H_2S and RSSH by MIMS. MIMS was carried out using a Hiden HPR-40 system containing a 20 mL sample cell and a membrane selective for detecting gases dissolved

https://dx.doi.org/10.1021/acs.joc.0c02412
J. Org. Chem. 2021, 86, 868−877

in aqueous solution. The sample cell was filled with 20 mL of PBS (pH 7.4, 100 mM) containing DTPA (100 μM) and purged with argon for at least 30 min prior to analysis. A stock solution of AS was prepared in 10 mM NaOH. A preweighed solid sample of Na_2S was dissolved in PBS to obtain the desired concentration of H_2S in solution. Hydropersulfide precursor and thiol stock solutions were prepared in DMSO. These stock solutions were purged with nitrogen for 10 min and used shortly after preparation. Aliquots (200 μL) of these solutions were injected into the sample cell using a gastight syringe and masses of interest were monitored with continuous sampling in positive ion mode.

4.4. GC Headspace Analysis of HNO Reaction with H_2S and RSSH. Hydropersulfide precursor and thiol stock solutions were prepared in DMSO. In order to compare the inherent nucleophilicity of the hydropersulfide compared to its thiol counterpart, the concentrations of hydropersulfide and thiol were corrected to have the same amount of anion present in solution. As the pK_a values of hydropersulfides are not known, it was assumed to be 1.5 units lower than the determined thiol pK_a. In a 15 mL vial sealed with rubber septum, 5 mL PBS (pH 7.4, 100 mM) containing DTPA (100 μM) was purged with argon for 25 min. These vials were placed in a heated cell block, which was held at 37 °C. The Na_2S or RSSH precursor or thiol and AS solutions were added to each vial to obtain 5 mL total volume, and the resulting solutions were incubated for 2 h at 37 °C. Headspace gas samples (60 μL) were injected into Agilent 8860 GC attached with Restek column (ShinCarbon ST 80/100, 2m, 1/8″ OD) to analyze N_2O. These experiments were carried out in triplicate for each concentration of interest and three injections were performed for each vial.

4.5. Analysis of Polysulfides by UPLC−MS. Polysulfides generated from the reaction of H_2S with HNO were analyzed by trapping with HPE-IAM by UPLC−MS. The reaction was performed in a 20 mL scintillation vial with a total reaction volume of 3 mL. H_2S (1 equiv) was incubated with various concentrations of AS (0.25 or 4 equiv) in freshly prepared ammonium bicarbonate buffer (pH 7.4, 50 mM) containing DTPA (100 μM). A 200 μL aliquot was taken from the reaction mixture at specified times and added to a solution of HPE-IAM (10 equiv) in ammonium bicarbonate buffer and incubated for 30 min. The samples were then loaded into vials in an autosampler maintained at 4 °C and analyzed using UPLC−MS as follows. Mobile phase: 0−1 min 90% water + 0% ACN + 10% formic acid (0.1%); 1−7.5 min gradient up to 10% water + 80% ACN + 10% formic acid (0.1%); 7.5−8.4 min 10% water + 80% ACN + 10% formic acid (0.1%); 8.4−8.5 min gradient up to 90% water + 0% ACN + 10% formic acid (0.1%); and 8.5−10 min 90% water + 0% ACN + 10% formic acid (0.1%). Flow rate = 0.3 mL min^{-1}. Similarly, various RSS_nSR and RSS−NH−S_nR species produced from the reaction of RSSH with HNO were analyzed by UPLC−MS. The mass signals for bis-(S)$_n$-HPE-IAM, (S)$_n$SR, and RS−NH−(S)$_n$R were obtained via deconvolution using MassLynx 4.1 software.

4.6. Hydroxylamine Analysis. An HPLC-based assay has been used for the detection of hydroxylamine (NH_2OH) by derivatization with vanillin.[50] We used this assay with slight modification. Briefly, H_2S (400 μM) was incubated with AS (100 μM) in pH 7.4 PBS (100 mM, 2 mL total volume) containing DTPA (100 μM) for 30 min at 37 °C. This mixture was then incubated with 4-cyanobenzaldehyde (1 mM) in pH 5.5 sodium acetate buffer (100 mM) for 2 h at 37 °C to convert NH_2OH to 4-cyanobenzaldehyde oxime. The resulting mixture was analyzed by Agilent high-performance liquid chromatography (HPLC). HPLC method—mobile phase A: water, and mobile phase B: ACN, flow rate: 1 mL/min, run time: 24 min, and the gradient elution method: 10 to 25% B from 0 to 18 min, 25 to 90% B from 18 to 24 min. Detection wavelengths: 254 and 268 nm. Column: Hichrom C-18 reversed phase column (150 mm × 4.6 mm, 5 μm).

4.7. Analysis of S_8 Using a Triphenylphosphine-^{31}P NMR-Based Assay. A white precipitate formed in the reaction of H_2S with HNO was analyzed using a triphenylphosphine (PPh_3)-based ^{31}P NMR assay. In a 20 mL scintillation vial, Na_2S (5 mM) was incubated with AS (20 mM) in ammonium bicarbonate buffer (pH 7.4, 50 mM) containing DTPA (100 μM) (final volume 5 mL) for 2 h at 37 °C. The reaction mixture was then extracted with $CDCl_3$ (1.5 mL × 3). To this, 500 μL of PPh_3 (50 mM, stock solution prepared in $CDCl_3$) was added and the resulting solution was incubated overnight at rt in a sealed vial. An internal standard triphenyl phosphate (1 mM) was added to the reaction mixture and analyzed using ^{31}P NMR spectrometry. A calibration curve was generated by reacting known amounts of commercially available sulfur (S_8) with equimolar amounts of PPh_3 along with 1 mM O=P(OPh)$_3$ as an internal standard. ^{31}P NMR spectra were acquired in $CDCl_3$ on a Bruker AVANCE I 400 MHz UltraShield NMR spectrometer.

4.8. Analysis of S_8 by EI-MS. As a second method of confirmation, the white precipitate produced from the reaction of H_2S with HNO (4 equiv) was analyzed by EI-MS. In a 20 mL scintillation vial, a reaction mixture was prepared with a final concentration of 2 mM Na_2S and 8 mM AS having a final reaction volume of 10 mL in pH 7.4 PBS (100 mM) containing DTPA (100 μM). The reaction was allowed to proceed until completion (approximately 2−3 h) and was then extracted with chloroform (1.5 mL × 3). The solvent was evaporated under vacuum to yield a white solid that was analyzed by EI-MS.

■ ASSOCIATED CONTENT

Supporting Information

The Supporting Information is available free of charge at https://pubs.acs.org/doi/10.1021/acs.joc.0c02412.

UV−vis spectra, HPLC traces, GC chromatograms, EI-MS analysis, UPLC−MS traces, mass spectra, and ^{31}P NMR spectra (PDF)

■ AUTHOR INFORMATION

Corresponding Author

John P. Toscano − *Department of Chemistry, Johns Hopkins University, Baltimore, Maryland 21218, United States;* orcid.org/0000-0002-4277-3533; Email: jtoscano@jhu.edu

Authors

Jessica Zarenkiewicz − *Department of Chemistry, Johns Hopkins University, Baltimore, Maryland 21218, United States*

Vinayak S. Khodade − *Department of Chemistry, Johns Hopkins University, Baltimore, Maryland 21218, United States;* orcid.org/0000-0003-2406-5856

Complete contact information is available at: https://pubs.acs.org/10.1021/acs.joc.0c02412

Author Contributions

†J.Z. and V.S.K. contributed equally.

Notes

The authors declare no competing financial interest.

■ ACKNOWLEDGMENTS

We gratefully acknowledge the National Science Foundation (CHE-1900285) for generous support for this research.

■ REFERENCES

(1) Paolocci, N.; Katori, T.; Champion, H. C.; St John, M. E.; Miranda, K. M.; Fukuto, J. M.; Wink, D. A.; Kass, D. A. Positive inotropic and lusitropic effects of HNO/NO$^-$ in failing hearts: Independence from β-adrenergic signaling. *Proc. Natl. Acad. Sci. U.S.A.* **2003**, *100*, 5537−5542.

(2) Paolocci, N.; Saavedra, W. F.; Miranda, K. M.; Martignani, C.; Isoda, T.; Hare, J. M.; Espey, M. G.; Fukuto, J. M.; Feelisch, M.; Wink, D. A.; Kass, D. A. Nitroxyl anion exerts redox-sensitive positive

cardiac inotropy *in vivo* by calcitonin gene-related peptide signaling. *Proc. Natl. Acad. Sci. U.S.A.* **2001**, *98*, 10463−10468.
(3) Norris, A. J.; Sartippour, M. R.; Lu, M.; Park, T.; Rao, J. Y.; Jackson, M. I.; Fukuto, J. M.; Brooks, M. N. Nitroxyl inhibits breast tumor growth and angiogenesis. *Int. J. Cancer* **2008**, *122*, 1905−1910.
(4) DeMaster, E. G.; Redfern, B.; Nagasawa, H. T. Mechanisms of Inhibition of Aldehyde Dehydrogenase by Nitroxyl, the Active Metabolite of the Alcohol Deterrent Agent Cyanamide. *Biochem. Pharmacol.* **1998**, *55*, 2007−2015.
(5) Bartberger, M. D.; Fukuto, J. M.; Houk, K. N. On the acidity and reactivity of HNO in aqueous solution and biological systems. *Proc. Natl. Acad. Sci. U.S.A.* **2001**, *98*, 2194−2198.
(6) Doyle, M. P.; Mahapatro, S. N.; Broene, R. D.; Guy, J. K. Oxidation and reduction of hemoproteins by trioxodinitrate(II). The role of nitrosyl hydride and nitrite. *J. Am. Chem. Soc.* **1988**, *110*, 593−599.
(7) Wong, P. S.-Y.; Hyun, J.; Fukuto, J. M.; Shirota, F. N.; DeMaster, E. G.; Shoeman, D. W.; Nagasawa, H. T. Reaction between S-Nitrosothiols and Thiols: Generation of Nitroxyl (HNO) and Subsequent Chemistry. *Biochemistry* **1998**, *37*, 5362−5371.
(8) Bianco, C. L.; Toscano, J. P.; Bartberger, M. D.; Fukuto, J. M. The chemical biology of HNO signaling. *Arch. Biochem. Biophys.* **2017**, *617*, 129−136.
(9) Miranda, K. M.; Paolocci, N.; Katori, T.; Thomas, D. D.; Ford, E.; Bartberger, M. D.; Espey, M. G.; Kass, D. A.; Feelisch, M.; Fukuto, J. M.; Wink, D. A. A biochemical rationale for the discrete behavior of nitroxyl and nitric oxide in the cardiovascular system. *Proc. Natl. Acad. Sci. U.S.A.* **2003**, *100*, 9196−9201.
(10) Jackson, M. I.; Han, T. H.; Serbulea, L.; Dutton, A.; Ford, E.; Miranda, K. M.; Houk, K. N.; Wink, D. A.; Fukuto, J. M. Kinetic feasibility of nitroxyl reduction by physiological reductants and biological implications. *Free Radicals Biol. Med.* **2009**, *47*, 1130−1139.
(11) Sherman, M. P.; Grither, W. R.; McCulla, R. D. Computational Investigation of the Reaction Mechanisms of Nitroxyl and Thiols. *J. Org. Chem.* **2010**, *75*, 4014−4024.
(12) Keceli, G.; Toscano, J. P. Reactivity of Nitroxyl-Derived Sulfinamides. *Biochemistry* **2012**, *51*, 4206−4216.
(13) Abe, K.; Kimura, H. The possible role of hydrogen sulfide as an endogenous neuromodulator. *J. Neurosci.* **1996**, *16*, 1066−1071.
(14) Stipanuk, M. H.; Beck, P. W. Characterization of the enzymic capacity for cysteine desulphhydration in liver and kidney of the rat. *Biochem. J.* **1982**, *206*, 267−277.
(15) Kabil, O.; Banerjee, R. Redox Biochemistry of Hydrogen Sulfide. *J. Biol. Chem.* **2010**, *285*, 21903−21907.
(16) Polhemus, D. J.; Lefer, D. J. Emergence of Hydrogen Sulfide as an Endogenous Gaseous Signaling Molecule in Cardiovascular Disease. *Circ. Res.* **2014**, *114*, 730−737.
(17) Gadalla, M. M.; Snyder, S. H. Hydrogen sulfide as a gasotransmitter. *J. Neurochem.* **2010**, *113*, 14−26.
(18) Kimura, H. Hydrogen sulfide: its production, release and functions. *Amino Acids* **2011**, *41*, 113−121.
(19) Guo, F.-F.; Yu, T.-Z.; Hong, J.; Fang, J.-Y. Emerging Roles of Hydrogen Sulfide in Inflammatory and Neoplastic Colonic Diseases. *Front. Physiol.* **2016**, *7*, 156.
(20) Hughes, M. N.; Centelles, M. N.; Moore, K. P. Making and working with hydrogen sulfide: The chemistry and generation of hydrogen sulfide in vitro and its measurement in vivo: a review. *Free Radicals Biol. Med.* **2009**, *47*, 1346−1353.
(21) Mustafa, A. K.; Gadalla, M. M.; Sen, N.; Kim, S.; Mu, W.; Gazi, S. K.; Barrow, R. K.; Yang, G.; Wang, R.; Snyder, S. H. H_2S Signals Through Protein S-Sulfhydration. *Sci. Signal.* **2009**, *2*, ra72.
(22) Fukuto, J. M.; Lin, J.; Khodade, V. S.; Toscano, J. P. Predicting the Possible Physiological/Biological Utility of the Hydropersulfide Functional Group Based on Its Chemistry: Similarities Between Hydropersulfides and Selenols. *Antioxid. Redox Signal.* **2020**, *33*, 1295−1307.
(23) Álvarez, L.; Bianco, C. L.; Toscano, J. P.; Lin, J.; Akaike, T.; Fukuto, J. M. Chemical Biology of Hydropersulfides and Related Species: Possible Roles in Cellular Protection and Redox Signaling. *Antioxid. Redox Signal.* **2017**, *27*, 622−633.
(24) Ida, T.; Sawa, T.; Ihara, H.; Tsuchiya, Y.; Watanabe, Y.; Kumagai, Y.; Suematsu, M.; Motohashi, H.; Fujii, S.; Matsunaga, T.; Yamamoto, M.; Ono, K.; Devarie-Baez, N. O.; Xian, M.; Fukuto, J. M.; Akaike, T. Reactive cysteine persulfides and S-polythiolation regulate oxidative stress and redox signaling. *Proc. Natl. Acad. Sci. U.S.A.* **2014**, *111*, 7606−7611.
(25) Akaike, T.; Ida, T.; Wei, F.-Y.; Nishida, M.; Kumagai, Y.; Alam, M. M.; Ihara, H.; Sawa, T.; Matsunaga, T.; Kasamatsu, S.; Nishimura, A.; Morita, M.; Tomizawa, K.; Nishimura, A.; Watanabe, S.; Inaba, K.; Shima, H.; Tanuma, N.; Jung, M.; Fujii, S.; Watanabe, Y.; Ohmuraya, M.; Nagy, P.; Feelisch, M.; Fukuto, J. M.; Motohashi, H. Cysteinyl-tRNA synthetase governs cysteine polysulfidation and mitochondrial bioenergetics. *Nat. Commun.* **2017**, *8*, 1177.
(26) Everett, S. A.; Folkes, L. K.; Wardman, P.; Asmus, K.-D. Free-Radical Repair by a Novel Perthiol: Reversible Hydrogen Transfer and Perthiyl Radical Formation. *Free Radic. Res.* **1994**, *20*, 387−400.
(27) Cuevasanta, E.; Lange, M.; Bonanata, J.; Coitiño, E. L.; Ferrer-Sueta, G.; Filipovic, M. R.; Alvarez, B. Reaction of Hydrogen Sulfide with Disulfide and Sulfenic Acid to Form the Strongly Nucleophilic Persulfide. *J. Biol. Chem.* **2015**, *290*, 26866−26880.
(28) Benchoam, D.; Semelak, J. A.; Cuevasanta, E.; Mastrogiovanni, M.; Grassano, J. S.; Ferrer-Sueta, G.; Zeida, A.; Trujillo, M.; Möller, M. N.; Estrin, D. A.; Alvarez, B. Acidity and nucleophilic reactivity of glutathione persulfide. *Biochem. Chem.* **2020**, *295*, 15466−15481.
(29) Everett, S. A.; Wardman, P. Perthiols as antioxidants: Radical-scavenging and prooxidative mechanisms. *Methods Enzymol.* **1995**, *251*, 55−69.
(30) Saund, S. S.; Sosa, V.; Henriquez, S.; Nguyen, Q. N. N.; Bianco, C. L.; Sosa, V.; Millikin, R.; White, C.; Le, H.; Ono, K.; Tantillo, D. J.; Kumagai, Y.; Akaike, T.; Lin, J.; Fukuto, J. M. The chemical biology of hydropersulfides (RSSH): Chemical stability, reactivity and redox role. *Arch. Biochem. Biophys.* **2015**, *588*, 15−24.
(31) Bianco, C. L.; Chavez, T. A.; Sosa, V.; Saund, S. S.; Nguyen, Q. N. N.; Tantillo, D. J.; Ichimura, A. S.; Toscano, J. P.; Fukuto, J. M. The chemical biology of the persulfide (RSSH)/perthiyl (RSS·) redox couple and possible role in biological redox signaling. *Free Radicals Biol. Med.* **2016**, *101*, 20−31.
(32) Millikin, R.; Bianco, C. L.; White, C.; Saund, S. S.; Henriquez, S.; Sosa, V.; Akaike, T.; Kumagai, Y.; Soeda, S.; Toscano, J. P.; Lin, J.; Fukuto, J. M. The chemical biology of protein hydropersulfides: Studies of a possible protective function of biological hydropersulfide generation. *Free Radicals Biol. Med.* **2016**, *97*, 136−147.
(33) Smith, P. A. S.; Hein, G. E. The Alleged Role of Nitroxyl in Certain Reactions of Aldehydes and Alkyl Halides1. *J. Am. Chem. Soc.* **1960**, *82*, 5731−5740.
(34) Bonner, F. T.; Ravid, B. Thermal decomposition of oxyhyponitrite (sodium trioxodinitrate(II)) in aqueous solution. *Inorg. Chem.* **1975**, *14*, 558−563.
(35) Hoch, G.; Kok, B. A mass spectrometer inlet system for sampling gases dissolved in liquid phases. *Arch. Biochem. Biophys.* **1963**, *101*, 160−170.
(36) Johnson, R. C.; Cooks, R. G.; Allen, T. M.; Cisper, M. E.; Hemberger, P. H. Membrane introduction Mass Spectrometry: Trends and applications. *Mass Spectrom. Rev.* **2000**, *19*, 1−37.
(37) Cline, M. R.; Tu, C.; Silverman, D. N.; Toscano, J. P. Detection of nitroxyl (HNO) by membrane inlet mass spectrometry. *Free Radicals Biol. Med.* **2011**, *50*, 1274−1279.
(38) Bogdándi, V.; Ida, T.; Sutton, T. R.; Bianco, C.; Ditrói, T.; Koster, G.; Henthorn, H. A.; Minnion, M.; Toscano, J. P.; van der Vliet, A.; Pluth, M. D.; Feelisch, M.; Fukuto, J. M.; Akaike, T.; Nagy, P. Speciation of reactive sulfur species and their reactions with alkylating agents: do we have any clue about what is present inside the cell? *Br. J. Pharmacol.* **2019**, *176*, 646−670.
(39) Hamid, H. A.; Tanaka, A.; Ida, T.; Nishimura, A.; Matsunaga, T.; Fujii, S.; Morita, M.; Sawa, T.; Fukuto, J. M.; Nagy, P.; Tsutsumi, R.; Motohashi, H.; Ihara, H.; Akaike, T. Polysulfide stabilization by tyrosine and hydroxyphenyl-containing derivatives that is important

https://dx.doi.org/10.1021/acs.joc.0c02412
J. Org. Chem. 2021, 86, 868−877

for a reactive sulfur metabolomics analysis. *Redox Biol.* **2019**, *21*, 101096.
(40) Bailey, T. S.; Zakharov, L. N.; Pluth, M. D. Understanding Hydrogen Sulfide Storage: Probing Conditions for Sulfide Release from Hydrodisulfides. *J. Am. Chem. Soc.* **2014**, *136*, 10573−10576.
(41) Kaba, R. A.; Ingold, K. U. Kinetic applications of electron paramagnetic resonance spectroscopy. 28. N-Alkoxy-N-alkylamino, N-alkoxyamino, and N-alkoxyanilino radicals. *J. Am. Chem. Soc.* **1976**, *98*, 7375−7380.
(42) Wallace, W. E. *NIST Chemistry WebBook NIST Standard Reference Database Number 69*; National Institute of Standards and Technology: Gaithersburg MD, 2014; Vol. *69*, p 20899.
(43) Filipovic, M. R.; Zivanovic, J.; Alvarez, B.; Banerjee, R. Chemical Biology of H_2S Signaling through Persulfidation. *Chem. Rev.* **2018**, *118*, 1253−1337.
(44) Khodade, V. S.; Pharoah, B. M.; Paolocci, N.; Toscano, J. P. Alkylamine-Substituted Perthiocarbamates: Dual Precursors to Hydropersulfide and Carbonyl Sulfide with Cardioprotective Actions. *J. Am. Chem. Soc.* **2020**, *142*, 4309−4316.
(45) Bailey, T. S.; Henthorn, H. A.; Pluth, M. D. The Intersection of NO and H_2S: Persulfides Generate NO from Nitrite through Polysulfide Formation. *Inorg. Chem.* **2016**, *55*, 12618−12625.
(46) Liu, H.; Radford, M. N.; Yang, C.-t.; Chen, W.; Xian, M. Inorganic hydrogen polysulfides: chemistry, chemical biology and detection. *Br. J. Pharmacol.* **2019**, *176*, 616−627.
(47) Hughes, M. N.; Cammack, R. Synthesis, chemistry, and applications of nitroxyl ion releasers sodium trioxodinitrate or Angeli's salt and piloty's acid. *Methods Enzymol.* **1999**, *301*, 279−287.
(48) Aizawa, K.; Nakagawa, H.; Matsuo, K.; Kawai, K.; Ieda, N.; Suzuki, T.; Miyata, N. Piloty's acid derivative with improved nitroxyl-releasing characteristics. *Bioorg. Med. Chem. Lett.* **2013**, *23*, 2340−2343.
(49) Tavares, A.; Schneider, P. H.; Merlo, A. A. 3,5-Disubstituted Isoxazolines as Potential Molecular Kits for Liquid-Crystalline Materials. *Eur. J. Org. Chem.* **2009**, 889−897.
(50) Korte, W. D. Determination of hydroxylamine in aqueous solutions of pyridinium aldoximes by high-performance liquid chromatography with UV and fluorometric detection. *J. Chromatogr. A* **1992**, *603*, 145−150.

https://dx.doi.org/10.1021/acs.joc.0c02412
J. Org. Chem. 2021, 86, 868−877